Available online at www.sciencedirect.com
ScienceDirect
Journal of the European Ceramic Society 27 (2007) 1399–1404
www.elsevier.com/locate/jeurceramsoc

# Nanoindentation characterization of SiC-based ceramics

Stefano Guicciardi [a,*], Andrea Balbo [a], Diletta Sciti [a], Cesare Melandri [a], Giuseppe Pezzotti [b]

[a] *Institute of Science and Technology for Ceramics, National Research Council, Via Granarolo 64, I-48018 Faenza, Italy*
[b] *Department of Chemistry and Materials Technology, Kyoto Institute of Technology, Sakyo-ku, Matsugasaki, 606-8585 Kyoto, Japan*

Available online 13 June 2006

**Abstract**

Depth-sensing indentation tests were carried out on several SiC-based liquid-phase-sintered SiC ceramics characterized by different mean grain size spanning from 78 to 540 nm. The indentation tests were performed with peak loads ranging from 5 to 400 mN in order to investigate the property variation with the variation of the peak load and material microstructure. The values of indentation hardness and Young's modulus were calculated according to the models developed by Oliver and Pharr (O&P) and by Cheng and Cheng (C&C). According to the O&P model, the finest grained SiC ceramics did not show the indentation size effect (ISE) which was observed in the largest grained SiC ceramics. The grain-size dependence of the indentation hardness can be described by an inverse Hall–Petch relation. With the C&C model, the correlation of the indentation hardness with the peak load and the grain size was less evident. The indentation hardness calculated by the O&P model was lower than that calculated by the C&C model and in better agreement with the values of Vickers microhardness. The O&P indentation Young's modulus was higher than the C&C indentation Young's modulus but the latter was in very good agreement with the values measured by resonant frequency. For both models, the indentation Young's modulus was almost load-independent even if a dependence on the microstructure was observed.


*Keywords:* Hardness; Mechanical properties; Carbides; SiC; Nanoindentation

## 1. Introduction

Depth-sensing indentation (DSI) tests allow the measurement of properties like hardness and Young's modulus in a very small volume of a material.[1–3] In most of the models which were developed for inferring properties from the loading–unloading curves, the knowledge of contact area between the indenter and the material surface is necessary. One of the most used model for the determination of the contact area and properties calculation is that developed by Oliver and Pharr (O&P).[4] According to the first version of this model, which was based on an iterative procedure, the area function and the machine compliance can be resumed from tests at different peak loads in a homogeneous and isotropic material. From the known area function and the corrected loading–unloading data, the O&P model describes how to calculate the indentation hardness and the Young's modulus. However, it was subsequently discovered that the plastic properties of the material under study can modify the contact area between the material and indenter so that the contact area derived by the area function might not be the correct one.[5] This is mainly due to the pile-up of the displaced material around the indentation, particularly in soft metals. An indication of the tendency of a material to pile-up is the ratio of $h_f/h_{max}$, where $h_f$ is the final displacement at complete unloading and $h_{max}$ is the maximum depth penetration during a DSI test. In order to obtain reliable results from the O&P model, this ratio should be less than 0.7.[5] Recently, based on dimensional analysis and extensive finite elements calculations, Cheng and Cheng (C&C) developed an alternative model to derive indentation hardness and Young's modulus from loading–unloading curves which avoids the problem to determine the area function of the indenter.[6,7] According to these authors, their model should have some advantages over that of O&P[8]: some calculations are carried out considering the whole loading–unloading curve, and not just a single point as in the O&P model, and, for not considering the contact area, the final results should not be affected by the eventual pile-up or sink-in around the indentation site.

In this work, DSI tests were carried on SiC-based ceramics at several peak loads in the range 5–400 mN. The indentation hardness and the Young's modulus were calculated according to the O&P and C&C models. Being very hard and stiff, these materials should virtually allow the comparison between the values of indentation hardness and Young's modulus calculated with the two models in case of no pile-up. Moreover, the different mean

* Corresponding author. Tel.: +39 0546 699720; fax: +39 0546 46381.
*E-mail address:* stefano@istec.cnr.it (S. Guicciardi).

0955-2219/$ – see front matter © 2006 Elsevier Ltd. All rights reserved.
doi:10.1016/j.jeurceramsoc.2006.05.057

Table 1
Characteristics of the sintered SiC samples

| Sample label | Starting powder/mean particle size | Sample composition (wt%) | Sintering addition | Sample grain size (nm) |
|---|---|---|---|---|
| S540 | Starck BF12/230 nm | $90SiC + 6Al_2O_3 + 4Y_2O_3$ | Ultrasonic mixing | 540 ± 10 |
| S360 | Starck BF12/230 nm | $90SiC + 6Al_2O_3 + 4Y_2O_3$ | Coprecipitation | 360 ± 2 |
| S139 | Plasma synthesis/60 nm | $90SiC + 6Al_2O_3 + 4Y_2O_3$ | Ultrasonic mixing | 139 ± 7 |
| S78 | Laser synthesis/30 nm | $90SiC + 7Al_2O_3 + 3Y_2O_3$ | Ultrasonic mixing | 78 ± 8 |

Mean values ± 1 standard deviation when appropriate.

grain size of the SiC ceramics and the variation of the peak load should permit to investigate the hardness and Young's modulus trend with the microstructure and penetration depth according to the two different models. For a better assessment, the indentation values of hardness and Young's modulus were also compared to the bulk values of hardness and Young's modulus measured by Vickers microhardness and resonant frequency.

## 2. Materials and testing

Four different SiC ceramics were sintered by hot-pressing in vacuum. The starting powders were a commercial submicrometer powder (Starck BF12) and two laboratory-produced nanosized powders as described in Table 1. Yttria and allumina, in amount of 10 wt.%, were used in all the cases as sintering aids. Two different routes were used for the addition of the sintering aids to the commercial powder: ultrasonic mixing and coprecipitation. For the laboratory-produced powders, only ultrasonic mixing was used. The microstructures of the sintered samples are shown in Fig. 1 after plasma etching. The SiC grains (dark areas) are separated by a grain boundary film which is the residue of the liquid phase sintering medium. The amount of intergranular phase visible in Fig. 1 is slightly overestimated due to the etching technique. By image analysis, the mean grain sizes (m.g.s.) of the dense samples were calculated as 540 nm and 360 nm for the materials obtained from the commercial submicro-sized powder, and 139 nm and 78 nm for the materials obtained from the nano-sized powders, Table 1. In the following, for an easier identification, the samples have been labelled using their mean grain size, i.e. S540, S360, S139 and S78. More details on processing and characteristics of the materials are reported in[9] for sample S540,[10] for sample S360 and[11] for samples S78 and S139.

As reference bulk properties, hardness and Young's modulus were measured on these materials by conventional techniques. On a hardness tester (Zwick 3212, Zwick, Ulm, Germany), the Vickers microhardness was measured with an applied force of 9.81 N. The surfaces of the specimens were mechanically polished using diamond paste down to 0.25 μm. The final mean surface roughness, $R_a$, was about 0.02 μm in all the specimens. The Young's modulus was measured by resonant frequency on specimens 28 mm × 8 mm × 0.8 mm using a gain-phase

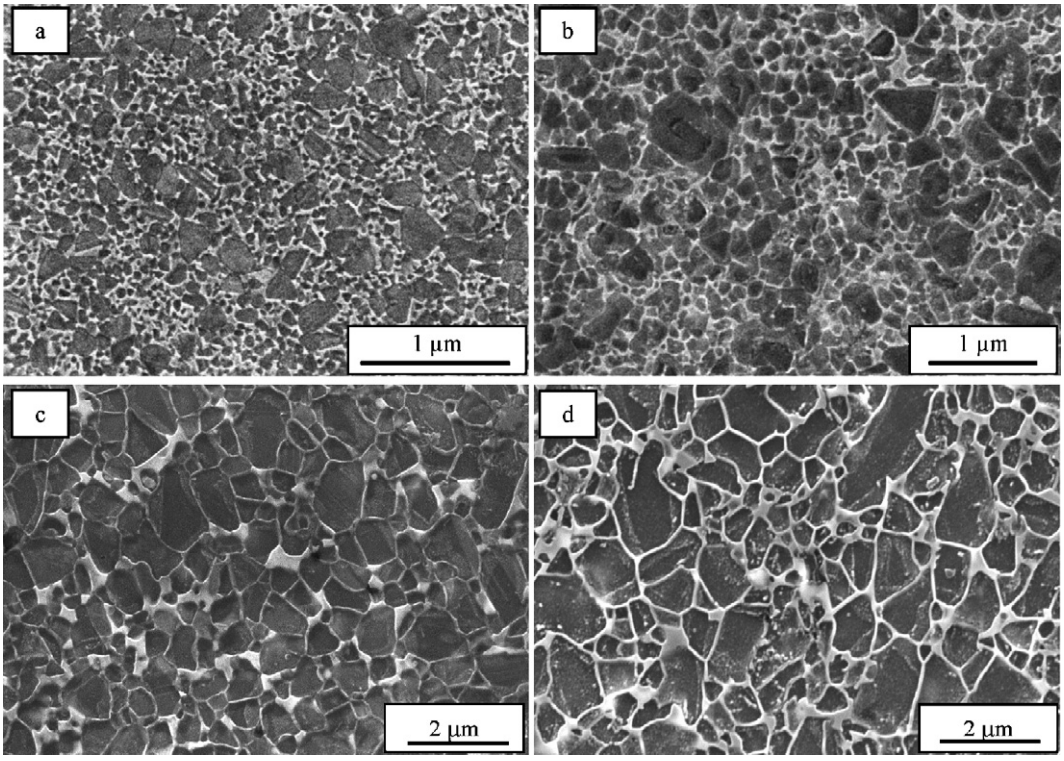


Fig. 1. SEM micrographs showing the microstructure of the samples. The surfaces were plasma-etched. (a) S78, (b) S139, (c) S360 and (d) S540.

analyzer (H&P 4194A, Yokogama, Hewlett Packard, Tokyo, Japan).

The depth-sensing indentation tests were performed in a nanoindenter (NanoIndenter XP™, MTS Systems Corporation, Oak Ridge, TN, USA) with a diamond Berkovich indenter. The polished SiC specimens were glued to aluminum cylinders. Six peak loads were used to investigate the indentation hardness and Young's modulus as a function of penetration depth: 5, 10, 50, 100, 200 and 400 mN. The indenter was loaded with a loading rate of 2.5 mN/s up to the peak load and unloaded with the same rate without holding time. For each peak load, at least ten indentations, spaced at 50 μm, were made. Indentation hardness ($H$) and Young's modulus ($E$) were calculated by the nanoindenter software TestWorks™ Ver. 4.06A based on the model of Oliver and Pharr.[4] In this software, the machine compliance and the thermal drift are automatically subtracted from the original raw data. $H^{OP}$ and $E^{OP}$ (OP superscript letters indicate the O&P model while in the following CC stand for the C&C model) of the tested material are calculated from the loading–unloading curves of the load, $P$, as a function of the displacement, $h$:

$$H^{OP} = \frac{P_{max}}{A_c}, \tag{1}$$

$$E^{OP} = \frac{1-\nu^2}{1/(E_r) - (1-\nu_i^2)/(E_i)}, \tag{2}$$

where $P_{max}$ is the peak load, $A_c$ the contact area, and $E^{OP}$, $E_i$, $\nu$ and $\nu_i$ are the Young's modulus and the Poisson ratio of the material and indenter, respectively ($E_i = 1141$ GPa and $\nu_i = 0.07$). $E_r$, the reduced Young's modulus, is calculated from the unloading data as

$$E_r = \frac{\sqrt{\pi}}{2} S \frac{1}{\beta} \frac{1}{\sqrt{A_c}}, \tag{3}$$

where $\beta$ is a constant equal to 1.034 for a Berkovich indenter and $S$ is the contact stiffness. The contact stiffness is calculated by fitting a percentage, 90% in our case, of the unloading data by a polynomial function and then taking the derivative of this function with respect to the displacement, i.e. d$P$/d$h$, and numerically evaluate it at the beginning of the unloading curve. In the O&P model, the contact area, $A_c$, is defined by a polynomial function $\left(A_c = \sum_{n=0}^{8} C_i h_c^{2-n}\right)$ of the contact depth, $h_c$, which is given by

$$h_c = h_{max} - \varepsilon \frac{P_{max}}{S}, \tag{4}$$

where $h_{max}$ is the displacement at the maximum load and $\varepsilon$ is a constant equal to 0.75. The coefficients $C_i$ of the area function are constants which must be determined by a least-squares procedure on indentation tests carried out at different peak loads on a standard sample with known load-independent Young's modulus.

For the calibration of the area function, DSI tests were carried out on a fused silica specimen with an indentation Young's modulus reference value of 72 GPa. Silica is usually chosen as reference material as it shows no pile-up or sink-in and its Young's modulus is load-independent. The peak load range for the calibration was chosen to encompass the contact depths which will be measured in the SiC samples. For the silica specimen, a Poisson ratio of 0.17 was taken. The number and the values of the $C_i$ coefficients were determined with the aid of a mathematical software (MATHEMATICA 5, Wolfram Inc., IL, USA). The best result, i.e. the minimum difference with respect to the reference value of 72 GPa, was obtained with an area function described by three coefficients with values $C_0 = 24.8172$, $C_1 = 463.793$, and $C_2 = 6.43024$. The results of this calibration are shown in Fig. 2.According to the C&C model, the indentation hardness ($H^{CC}$) and Young's modulus ($E^{CC}$) of a material can be calculated by the following equations[6,7]:

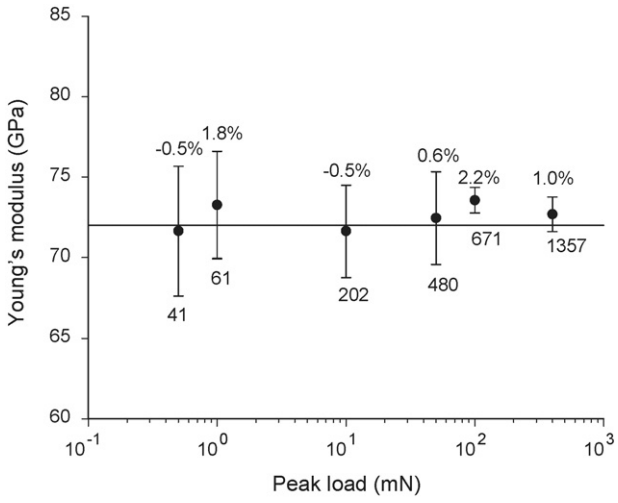


Fig. 2. Calibration results for the Young's modulus on the standard fused silica. Points and error bars are mean values ± 1 standard deviation, respectively. The upper figures refer to the percentage difference with respect to the reference value of 72 GPa indicated by the horizontal line. The lower figures refer to the calculated contact depth, $h_c$, in nm.

$$\frac{H^{CC}}{E_r} = \frac{1}{\lambda(1+\gamma)} \frac{W_{unl}}{W_{tot}}, \tag{5}$$

$$\frac{H^{CC}}{E_r^2} = \frac{4}{\pi} \frac{P_{max}}{S^2}, \tag{6}$$

where $\lambda = 0.27$ and $\gamma = 1.5 \tan\theta + 0.327$, respectively, $\theta$ is the semi-angle of the cone with an equivalent (area/penetration depth) ratio of the Berkovich indenter and can be estimated by the first coefficient of the area function, $C_0$, and $W_{tot}$ and $W_{unl}$ are the areas under the loading and unloading curves, respectively. The other symbols have the same meaning as above. The numerical integration of the loading and unloading curves was carried out using the mathematical software already indicated. For all the SiC materials, a Poisson's ratio of 0.19 was used.[12]

## 3. Results and discussion

### 3.1. Bulk properties

The values of Vickers microhardness and Young's modulus by resonant frequency of the four SiC samples are reported in

Table 2
Mechanical properties of the sintered SiC samples

| Sample label | Vickers1,0 hardness (GPa) | Resonant frequency Young's modulus (GPa) |
|---|---|---|
| S540 | 22.0 ± 0.8 | 386 |
| S360 | 23.2 ± 1.7 | 405 |
| S139 | 21.9 ± 0.3 | 334 |
| S78 | 21.9 ± 0.5 | 376 |

Mean values ± 1 standard deviation when appropriate.

Table 2. The higher mechanical properties of S360 are due to its low silica content in the grain boundary phase.[10] For the other SiC samples, it can be seen that the hardness is almost the same while the Young's modulus of S139 is lower than S540 and S78 due to a small amount of porosity (∼1 vol.%).[11]

### 3.2. O&P indentation hardness

As reported in the Introduction, the ratio $h_f/h_{max}$ can be taken as an indication of the tendency of the material to present pile-up around an indentation. In Fig. 3, this ratio is shown as a function of the peak load and material. As can be seen, $h_f/h_{max}$ is well lower than 0.7 in all the materials and for all the peak loads employed. In particular, no difference is observed for the $h_f/h_{max}$ ratio as a function of the material while a slight increasing trend with the peak load can be pointed out.

The indentation hardness calculated according to the O&P model is reported as a function of the peak load and material in Fig. 4(a). As general behavior, the mean values of S540 and S360 tend to decrease with the increase of the peak load (indentation size effect, ISE[15]). On the other hand, the SiC samples with the smallest grain size, S139 and S78, show no evidence of ISE. For all the materials, the standard deviations are very high at low peak loads and decrease with the increasing of the peak load. This tendency seems to be independent on the sample microstructure. For high peak loads, the indentation hardness of the sample S540, S139 and S78 seems to converge to a common

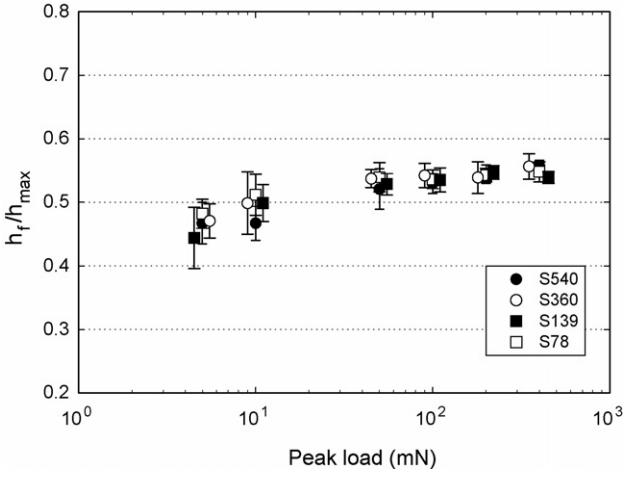


Fig. 3. Ratio between the penetration depth at complete unloading, $h_f$, and the maximum penetration depth, $h_{max}$, as a function of peak load and material. The points have been slightly shifted for better readability.

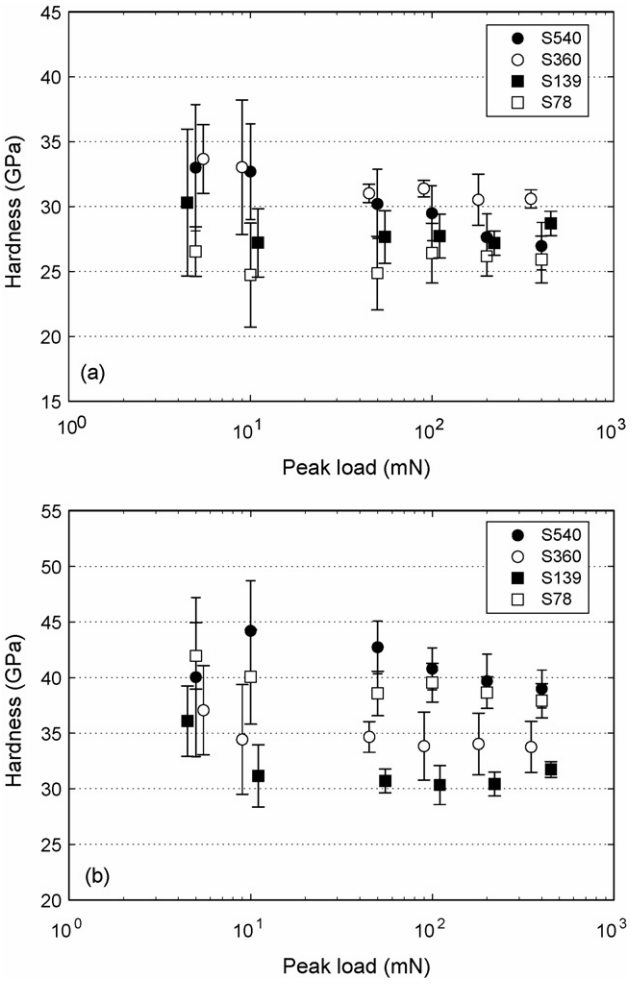


Fig. 4. Plot of the hardness as a function of the peak load and material calculated according to the model of Oliver and Pharr (a) and Cheng and Cheng (b). Points and bars represent mean values and ±1 standard deviation. The points have been slightly shifted for better readability.

value. This was interpreted as the consequence of the influence of the microstructural scale when the penetration depth was comparable to the m.g.s. of the material.[16]

When tested at the same peak load, the indentation hardness of the SiC ceramics decreases with the decreasing of the m.g.s. of the material, indicating that in this grain size range the hardness can obey an inverse Hall–Petch relation.[17] Sample S360, which is the hardest by O&P nanoindentation and Vickers microhardness, does not follow this relation very likely for its low silica-content grain boundary phase.[10] The O&P indentation hardness values are higher that the Vickers microhardness for all the SiC samples but the relative ranking is confirmed, especially at high peak loads. The higher values of the O&P indentation hardness with respect to the Vickers microhardness are very likely due to the much smaller deformed volumes which hardly contain defects promoting plastic deformation like microcracks or micropores. An ulterior contribution to the difference between the two measurements can be due to an eventual presence of pile-up around the indentations which influences the results. In fact, even if a $h_f/h_{max}$ ratio lower than 0.7 was indicated as a safety region for excluding pile-up,[5]

the experimental investigations in advanced structural ceramics do not completely confirm this as in a $Si_3N_4$-based ceramic a slight pile-up around nanoindentations was observed in[13] but not in.[14]

### 3.3. C&C indentation hardness

The indentation hardness of the SiC samples calculated according to the model of C&C is shown in Fig. 4(b). The mean values are even higher, and the standard deviations larger, than those calculated by the O&P model. The ISE in the largest grained ceramics, S540 and S360, is much less evident than in the case of O&P indentation hardness. For peak loads higher than 5 mN, in fact, all the SiC samples have an almost constant value with only S540 showing a slight decrease with the increasing of the peak load. At 5 mN, the indentation hardness of S540 decreases and those of S360 and S139 increase.

In correspondence of the same peak load, the C&C indentation hardness does not show any clear dependence on the grain size and the C&C model does not maintain the relative ranking among the materials as measured by the O&P model and Vickers microhardness.

Considering the Vickers microhardness reported in Table 2 as reference values, it can be noted that the agreement with the Vickers microhardness is better in the case of the O&P model than in the case of the C&C model, both for the absolute indentation hardness values and for the relative ranking among the materials.

### 3.4. O&P indentation Young's modulus

The O&P indentation Young's modulus of the four SiC samples as a function of peak load and material is shown in Fig. 5(a). The dependency of the indentation Young's modulus on the peak load is either absent, as in the case of S360, S139 and S78, or non-monotonous as for S540. Also for this property, the standard deviation decreases with the increase of the peak load. For high peak loads, the indentation Young's modulus of samples S540, S139 and S78 converges to a common value. As for the indentation hardness, the scale ratio between the m.g.s. of the material and the penetration depth was proposed as an explanation of this phenomenon.[16]

When compared to the values by resonant frequency reported in Table 2, it can be seen that the O&P model gives higher values with an overestimation in the range between 6% (S78) and 22% (S139). The possible presence of pile-up around the nanoindentations can explain this difference. The low amount of porosity which affects the bulk Young's modulus of S139 does not play a role in the indentation Young's modulus as this value is comparable to those of S540 and S78. It is very likely that, being a very local measurement, the nanoindentation values are not affected by the presence of a dilute porosity which instead influences the resonant frequency method. The stiffer grain boundary phase of sample S360 makes the indentation Young's modulus of this material higher than those of the other samples, in agreement with the reference bulk values, Table 2.

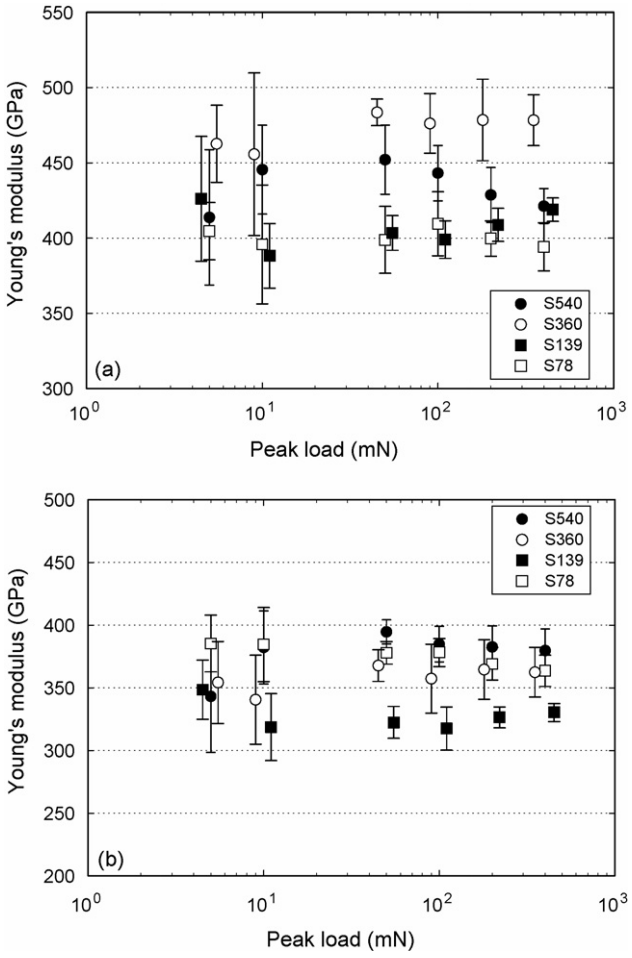


Fig. 5. Plot of the Young's modulus as a function of the peak load and material calculated according to the model of Oliver and Pharr (a) and Cheng and Cheng (b). Points and bars represent mean values and ±1 standard deviation. The points have been slightly shifted for better readability.

### 3.5. C&C indentation Young's modulus

The indentation Young's modulus as a function of peak load and material calculated according to the C&C model is shown in Fig. 5(b). As already found for the hardness, the C&C values are different than those calculated by the O&P model but in this case the C&C values are lower than the O&P ones. The Young's modulus is almost load-independent for all the SiC samples, as for the O&P model. However, the relative ranking among the samples is not maintained when passing from the O&P model to the C&C model. The values of indentation Young's modulus of the samples S540, S139 and S78 are in a very good agreement with those measured by resonant frequency, Table 2. Only the expected high value of sample S360 due to its low silica-content is not confirmed by the C&C model. The reasons of that are not clear at the moment.

## 4. Conclusions

Four SiC ceramics, with mean grain size ranging from 78 to 540 nm, were characterized by depth-sensing indentation tests. Several peak loads were used to study the variation of the inden-

tation hardness and Young's modulus with the penetration depth. The values of indentation hardness and Young's modulus were calculated according to the models developed by Oliver and Pharr (O&P) and by Cheng and Cheng (C&C).

With the O&P model, the indentation hardness values were lower than those calculated by the C&C model. With the O&P model, the largest grained SiC ceramics showed an indentation size effect which was not observed in the finest SiC samples. For the grain size range investigated, an inverse Hall–Petch relation seems to hold. The trend of the C&C indentation hardness was less load- and microstructure-dependent. The values calculated with the O&P model were in a better agreement with the values of Vickers microhardness.

For the indentation Young's modulus, the O&P model gave higher values than the C&C model and the resonant frequency method. The O&P ranking of the SiC ceramics was relatively good: the stiffest material as measured by resonant frequency was also the stiffest by the O&P method. However, very likely for its local nature, the small amount of porosity of a sample was ignored and its indentation Young's modulus was not the lowest as for the resonant frequency method. Most of the indentation Young's moduli measured according to the C&C model were in good agreement with the reference Young's modulus measured by resonant frequency. In particular, the C&C model correctly individuated the material with the lowest Young's modulus as measured by the resonant frequency method. On the other hand, the C&C model did not correctly rank the material which was the stiffest by resonant frequency method.

## References


1. Blau, P. and Lawn, B. R. ed., *Microindentation Techniques in Materials Science and Engineering*, *American Society for Testing and Materials*. ASTM STP, Philadelphia, 1986.
2. Focus topic: nanoindentation. *J. Mater. Res.*, 1999, **14**, 2196–2350.
3. Focus topic: nanoindentation. *J. Mater. Res.*, 2004, **19**, 3–395.
4. Oliver, W. C. and Pharr, G. M., An improved technique for determining hardness and elastic modulus using load and displacement sensing indentation experiments. *J. Mater. Res.*, 1992, **7**, 1564–1583.
5. Bolshakov, A. and Pharr, G. M., Influences of pileup on the measurement of mechanical properties by load and depth sensing indentation techniques. *J. Mater. Res.*, 1998, **13**, 1049–1058.
6. Cheng, Y.-T. and Cheng, C.-M., Relationship between hardness, elastic modulus and the work of indentation. *Appl. Phys. Lett.*, 1998, **73**, 614–616.
7. Cheng, Y.-T., Li, Z. and Cheng, C.-M., Scaling relationships for indentation measurements. *Phil. Mag. A*, 2002, **10**, 1821–1829.
8. Cheng, Y.-T. and Cheng, C.-M., Scaling, dimensional analysis, and indentation measurements. *Mater. Sci. Eng. R*, 2004, **44**, 91–149.
9. Sciti, D. and Bellosi, A., Effect of additives on densification, microstructure and properties of liquid-phase-sintered silicon carbide. *J. Mater. Sci.*, 2000, **35**, 1–7.
10. Sciti, D., Balbo, A. and Bellosi, A., Improvements offered by coprecipitation of sintering additives on ultra-fine SiC materials. *Adv. Eng. Mater.*, 2005, **7**, 152–158.
11. Sciti, D., Vicens, J., Herlin, N., Grabis, J. and Bellosi, A., SiC nano-materials produced through liquid phase sintering: processing and properties. *J. Ceram. Proc. Res.*, 2004, **5**, 40–47.
12. Shackelford, J. F. and Alexander, W., ed., *CRC Materials Science and Engineering Handbook*. CRC Press, USA, 2001.
13. Suganuma, M. and Swain, M. V., Simple method and critical comparison of frame compliance and indenter area function for nanoindentation. *J. Mater. Res.*, 2004, **19**, 3490–3502.
14. Lim, Y. Y. and Chaudhri, M. M., Do residual nanoindentations in metals and ceramics relax with time? *J. Phys. D: Appl. Phys.*, 2001, **34**, L70–L78.
15. MacColm, I. J., *Ceramic Hardness*. Plenum Press, New York, USA, 1990.
16. Guicciardi, S., Sciti, D., Melandri, C. and Bellosi, A., Nanoindentation characterization of submicro- and nano-sized liquid-phase-sintered SiC ceramics. *J. Am. Ceram. Soc.*, 2004, **87**, 2101–2107.
17. Konstantinidis, D. A. and Aifantis, E. C., On the anomalous hardness of nanocrystalline materials. *Nanostruct. Mater.*, 1998, **10**, 1111–1118.